Proc. NIPR Symp. Antarct. Meteorites, 4, 404–419, 1991

TETRATAENITE IN CHONDRITES AND EXPERIMENTAL DEMONSTRATION ON FORMATION OF TETRATAENITE FINE GRAINS

Takesi NAGATA[1], Chihiro KAITO[2], Yoshio SAITO[2] and Minoru FUNAKI[1]

[1]*National Institute of Polar Research, 9–10, Kaga 1-chome, Itabashi-ku, Tokyo 173*
[2]*Physics Department, Kyoto Technical University, Kyoto 606*

Abstract: Tetrataenite ($Fe_{50}Ni_{50}\gamma''$ phase) is a unique metallic mineral in meteorites. A magnetic granulometry analysis of chondrites on the basis of magnetic hysteresis parameters at various temperatures has shown that some LL chondrites contain very fine grains of tetrataenite metal, the grain sizes of which are 10 nm or smaller in diameter.

The coalescence growth process of a joint cloud of fine smoke particles evaporated from Fe and that from Ni produces fine grains of tetrataenite (FeNi γ''), in addition to those of ordered kamacite (Fe_3Ni), awaruite ($FeNi_3$) as well as disordered taenites. An outline of the experimental procedures of coalescence growth formation of tetrataenite and the other ordered crystal grains of Fe-Ni alloy and main results of the experiments is described.

1. Introduction

As already reported (NAGATA and FUNAKI, 1982, 1987, 1989; NAGATA *et al.*, 1986; NAGATA, 1988), chondrites whose metallic components are rich in Ni content, often contain the tetrataenite (FeNi γ'') phase which has a large crystalline anisotropy owing to its tetragonal crystal structure, so that its magnetic coercivity also is unusually large.

Among the tetrataenite-rich chondrites studied so far, the metallic components in Olivenza (LL6) and St. Séverin (LL6) chondrites contain tetrataenite as much as about 40 and 50 wt % respectively, as exemplified by the results of their Mössbauer spectral analysis (NAGATA *et al.*, 1986).

Grain sizes of the tetrataenite phase in chondrites are generally very small. For example, the mean diameter of tetrataenite in the St. Séverin, observable by a scanning electron micrograph ($\times 20000$), mostly ranges between 150 and 300 nm (DANON *et al.*, 1979). A problem concerned in the present study is how these small metallic grains of the special ordered crystal structure of AuCu type of tetrataenite, which has FeNi in chemical composition, could be formed in the environmental conditions of the solar nebula.

A single crystal of tetrataenite was first artificially produced by neutron irradiation of a single crystal of disordered taenite in the presence of a magnetic field of 2500 Oe along the (100) axis at 295°C, where the total neutron flux is 1.5×10^{20} neutron cm^{-2} and the energy of about 15% of the neutron flux is larger than 1 MeV (NÉEL

et al., 1964). The artificial formation of tetrataenite has also been experimentally demonstrated by irradiating a disordered FeNi specimen by an electron beam of about 1 MeV in energy (*e. g.*, CHAMBEROD *et al.*, 1979).

It seems likely that these experimental results strongly suggest a possible formation mechanism of the tetrataenite phase in iron meteorites such as Santa Catharina Ni-rich ataxite or taenite lamellae of Toluca octahedrite, for example (NAGATA *et al.*, 1987), where the effects of irradiation by neutrons or electrons are assumed to be equivalent to those of thermal agitations during an extremely long period of time, namely $10^6 \sim 10^8$ years.

In the case of the tetrataenite phase in fine metallic grains in chondrites, particularly the tetrataenite phase occupying nearly a half of individual metallic grains on average, however, it appears that further considerations may be needed for explaining plausible processes to form a large number of fine Fe-Ni grains containing a considerable share of tetrataenite, which are scattered within assemblages of chondritic silicate minerals.

On the other hand, AuCu alloy fine particles are experimentally produced successfully by coalescence of Au and Cu smoke streams in inert gas atmosphere of adequate pressure (KAITO, 1984). It appears possible, then, that tetrataenite, and probably other ordered Fe-Ni crystals such as awaruite ($FeNi_3$) also, can be formed by coalescence of Fe and Ni smoke streams. The present study deals with reasonably successful results of experimental formation of fine grains of tetrataenite and other ordered and disordered crystals of Fe-Ni alloy by coalescence of Fe and Ni smoke streams in inert gas, in comparison with the characteristics of tetrataenite fine grains contained in chondrites.

2. Magnetic Analysis and Magnetic Granulometry of Ferromagnetic Components in Ordinary Chondrites

Magnetic analysis method for meteorites consists of two main experimental procedures (*e. g.*, NAGATA *et al.*, 1986). One of the procedures is magnetic hysteresis cycle curve measurement at various temperatures (T) within the temperature range of ferromagnetic (or ferrimagnetic) components, which give the ferromagnetic hysteresis parameters such as saturation magnetization I_S (T), saturated isothermal remanent magnetization, $I_R(T)$, coercive force, $H_C(T)$, remanence coercive force, $H_{RC}(T)$ and paramagnetic susceptibility, $X_P(T)$. The other procedure is the determination of continuous thermomagnetic curves of $I_S(T)$ at least for the first heating and cooling temperature variation cycle, which give Curie point, Θ_C, magnetic phase transition temperature such as $\alpha \rightarrow \gamma$ transition at $T\alpha \rightarrow \gamma$ and $\gamma \rightarrow \alpha$ transition at $T\gamma \rightarrow \alpha$ of kamacite, and if any, a destruction or a formation of magnetic phase.

On the other hand, the magnetic constituents of ordinary chondrites can be approximately divided in many cases into two groups with respect to their magnetic coercivity; a high coercive component and a low coercive one. The high coercive component is either a group of tetrataenite which has a highly anisotropic crystal structure or Fe-Ni metal single-domain (SD) grains having a considerably large shape anisotropy, while the low coercive one is a group of disordered Fe-Ni metallic grains

Table 1a. Composition of metallic constituent in LL chondrites.

Chondrite	Mössbauer analysis (wt%) (T=25°C)			Magnetic analysis (wt%) (T=25°C)		
	α	γ	γ''	α	γ	γ''
Olivenza (LL6)	45	15	40	40	14	46
St. Séverin (LL6)	40	10	50	47	11	42
Appley Bridge (LL6)	~0	20~40	80~60	~0	57	43

Remarks α: Kamacite, γ: Disordered taenite, γ'': Tetrataenite.

Table 1b. Composition of metallic constituent in Tuxtuac LL5 chondrite.

Analysis method	α	γ (wt%)	γ''
(Original)			
Mössbauer	~0	85	15
Magnetic (25°C)	~0	100	~0
Magnetic (−269°C)	~0	91	9
(After heat treatment)			
Magnetic (25°C)	~0	100	~0
Magnetic (−269°C)	~0	100	~0

of multidomain structure. On the basis of the observed characteristics of magnetic coercivity spectrum of ordinary chondrites, a magnetic binary system model has been proposed for ordinary chondrites and achondrites (NAGATA and CARLETON, 1987). On the basis of the magnetic binary system model, the contents of tetrataenite and the other low coercivity components in chondrites have been estimated (NAGATA, 1988; NAGATA and CARLETON, 1989; NAGATA and FUNAKI, 1989). Examples thus obtained by the binary system analysis with the aid of the thermomagnetic analysis to identify the concerned ferromagnetic Fe-Ni metals are given in Table 1a together with the results of Mössbauer spectral analyses of separate specimens of the same chondrites for comparison, where α, γ and γ'' denote respectively kamacite, disordered taenite and tetrataenite. Table 1a shows that the results of magnetic analysis are in a roughly approximate agreement with those of Mössbauer spectral analysis, though samples examined in each case are different between the two analysis methods. In all cases of the three LL6 chondrites, tetrataenite phase (γ'') after heating up to 800°C has been transformed to the disordered taenite (γ) of the same chemical composition.

In another example shown in Table 1b, however, a magnetic analysis of Tuxtuac LL5 chondrite at 25°C shows that practically no tetrataenite phase is contained, though a Mössbauer analysis indicates that the tetrataenite content in the same chondrite amounts to about 15 wt% of metallic constituent. Since a magnetic analysis at the liquid helium temperature gives 9 wt% of tetrataenite in the metallic component of the same specimen, as shown in Table 1b, it may be evident that the tetrataenite phase in this chondrite is in the form of superparamagnetically fine particles at room temperature. The critical temperature (*Tb*), above which SD ferromagnetic fine grains behave paramagnetically and below which they behave ferromagnetically, is called the blocking temperature of ferromagnetic SD particles on the basis of Néel's

theory of superparamagnetism (NÉEL, 1949). In the theory the relaxation time (τ_0) of rotation of a uniaxially magnetized fine grain of V in volume and K_u in uniaxial anisotropy energy in a weak magnetic field is given by

$$1/\tau_0 = f_0 \exp(-K_u V/kT), \tag{1}$$

where k is Bolzmans' constant and f_0 is a pseud constant of $10^9\ s^{-1}$ in the order of magnitude, depending on material constants. In laboratory experiments an ensemble of the magnetic fine grains can be considered superparamagnetic when $\tau \ll 10^2 s \equiv \tau_0$, while it behaves ferromagnetically when $\tau \gg \tau_0$, thus the blocking temperature τ_0 being defined. If anisotropic energy $K_u(T)$ is known as a function of temperature (T), the distribution spectrum of $V(Tb)$ can be determined with the aid of eq. (1) from experimental data of magnetic hysteresis characteristics at various temperatures.

The magnetic granulometry method on the above-mentioned basis was discussed for the case of ensembles of fine grains of various sizes of a single magnetic phase in the lunar surface samples (SCHWERE and NAGATA, 1976). In the binary system model analysis of chondrites containing tetrataenite as the high coercivity component also, the basic principle of magnetic granulometry is applicable, provided that the dependence of K_u on temperature is known. The average coercive force H_C of an ensemble of independent grains oriented at random is expressed (*e.g.*, NAGATA, 1961) by

$$H_u = 0.958 K_u/J_S. \tag{2}$$

K_u and J_S (saturation magnetization) values of tetrataenite single crystal measured at room temperature are $K_u = 3.2\times10^6$ erg/cm^3 and $J_S = 1.3\times10^3$ emu/cm^3 respectively, while the observed value of H_C at 22°C of an ensemble of tetrataenite grains is 2250 Oe, which approximately satisfies eq. (2), as shown in Table 2.

Table 2. Dependence of magnetic hysteresis parameters and relative content in metal and coercive force of tetrataenite in Olivenza LL6 chondrite.

Temperature	−269	−200	−150	−100	−50	+22
I_S (emu/g)	3.05	2.50	2.49	2.49	2.48	2.42
I_R (emu/g)	0.895	0.790	0.770	0.774	0.770	0.746
H_C (Oe)	780	1125	1165	1190	1120	1245
H_{RC} (Oe)	4130	4100	3950	3890	3830	3810
m (wt%)	64.9	69.1	67.8	68.3	68.1	67.6
$H_C^{(h)}$ (Oe)	2765	2740	2640	2600	2560	2550
$H_C^{(l)}$ (Oe)	41	57	62	64	60	69
P (wt%)	1.11	0.98	0.96	0.96	0.96	0.93
V (cm^3)	4.90×10^{-21}	8.50×10^{-20}	1.44×10^{-19}	2.01×10^{-19}	2.60×10^{-19}	3.49×10^{-19}
l (nm)	1.70	4.04	5.24	5.86	6.38	7.04

(Remarks) m: Relative content of tetrataenite in metal.
$H_C^{(h)}$: Coercive force of high coercivity component (tetrataenite).
$H_C^{(l)}$: Coercive force of low coercivity component.
P: Bulk content of ferromagnetic tetrataenite.

Since $J_S(T)$ of tetrataenite is approximately constant within a temperature range between −269°C and 100°C (*e. g.*, NAGATA *et al.*, 1986), the dependence of $K_u(T)$ on temperature can be determined from measured values of $H_C(T)$ through eq. (2).

Magnetic hysteresis parameters, I_S, I_R, H_C and H_{RC} of a bulk sample of Olivenza LL6 chondrite obtained at various temperatures below 22°C, and coercive force $H_C^{(h)}$ of the high coercivity component (tetrataenite), $H_C^{(l)}$ of the low coercivity component (average of kamacite and disordered taenite) and relative content of tetrataenite in total metal (m), which are derived with the aid of the binary-system model analysis are summarized in Table 2. This result indicates that coercive force $H_C^{(h)}$ of tetrataenite component slightly increases with a decrease in temperature from 22°C to −269°C, but the total increase rate of $H_C^{(h)}$ from 22°C to −269°C is less than 10%. We may be able to consider therefore that $H_C^{(l)}$ is nearly constant whence $K_u(T)$ is approximately invariant within the same temperature range. Putting $\tau_0=10^2$ s, and $K_u=3.2\times10^6$ erg/cm^3 in eq. (1), throughout a temperature range between −270°C and +30°C, volume (V) of tetrataenite grains and $l\equiv V^{1/3}$ for a cubic model of the grains are evaluated for $T=Tb$ which corresponds to $\tau_0=10^2$ s in eq. (1) as summarized in Table 2, where the bulk content (P) of tetrataenite in ferromagnetic state also is given at each temperature.

As shown in Table 2, P value of this chondrite is kept nearly constant at temperatures below 22°C, so that $V>3.5\times10^{-19}$ cm^3 or $l>7$ nm for the absolute majority of tetrataenite grains in Olivenza LL6 chondrite. On the contrary, grain size of the majority of tetrataenite grains in Tuxtuac LL5 chondrite (Table 1b) is characterized by $V<3.5\times10^{-19}$ cm^3 or $l<7$ nm.

Another example of magnetic granulometry of fine grains of tetrataenite in chondrites is concerned with ultrafine grains of tetrataenite contained in silicate grains of matrix of St. Séverin LL6 chondrite. As already reported (NAGATA *et al.*, 1986), St. Séverin chondrite contains a large number of tetrataenite grains of 0.15∼0.3 μm in mean diameter, but apparent silicate grains of matrix of this chondrite also contain very fine grains of tetrataenite (NAGATA and FUNAKI, 1989). Figure 1 illustrates the dependence of P value on Tb of an ensemble of the silicate mineral grains containing fine tetrataenite particles of St. Séverin chondrite, derived by the same magnetic

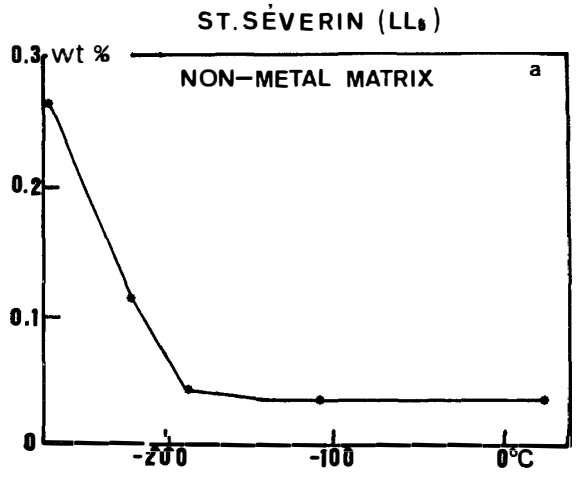

Fig. 1. Bulk content of ferromagnetic tetrataenite in silicate component of St. Séverin LL6 chondrite at low temperatures. (Grain sizes of tetrataenite, whose blocking temperatures are −200°C, −100°C and 0°C, are 4.4, 5.9 and 6.8 nm, respectively in mean diameter).

granulometry analysis. This result indicates that St. Séverin chondrite contains very fine grains of tetrataenite represented by $Tb < -200°C$ or $l < 4.4$ nm.

3. Experimental Formation of Tetrataenite and Other Fe-Ni grains of Ordered Crystal Structure by Coalescence of Fe and Ni Smoke Grains

One of the experimental methods to produce ultrafine grains may be the "gas evaporation technique", in which a solid material is heated in inert gas atmosphere (KIMOTO *et al.*, 1963). The heated vapor is subsequently cooled and condensed in the gas atmosphere, resulting in a smoke press which looks like the flame of a candle. Evidence for, and mechanism involved in the coalescence growth of the resulting smoke particles have been elucidated in a series of experiments (KAITO, 1978, 1981, 1984, 1985). The coalescence process takes place during a short period of time such as $10^{-3} \sim 10^{-2}$ s, and a joint smoke of two different metallic elements can form ordered grains of their alloy in an appropriate condition.

A formation of tetrataenite (FeNi γ'') fine grains also is possible by the present gas-evaporation-coalescence technique from Fe- and Ni-evaporated smokes. The gas-evaporation-coalescence system is schematically shown in Fig. 2. The sample preparation chamber is a glass cylinder of 17 cm in inner diameter and 33 cm in height

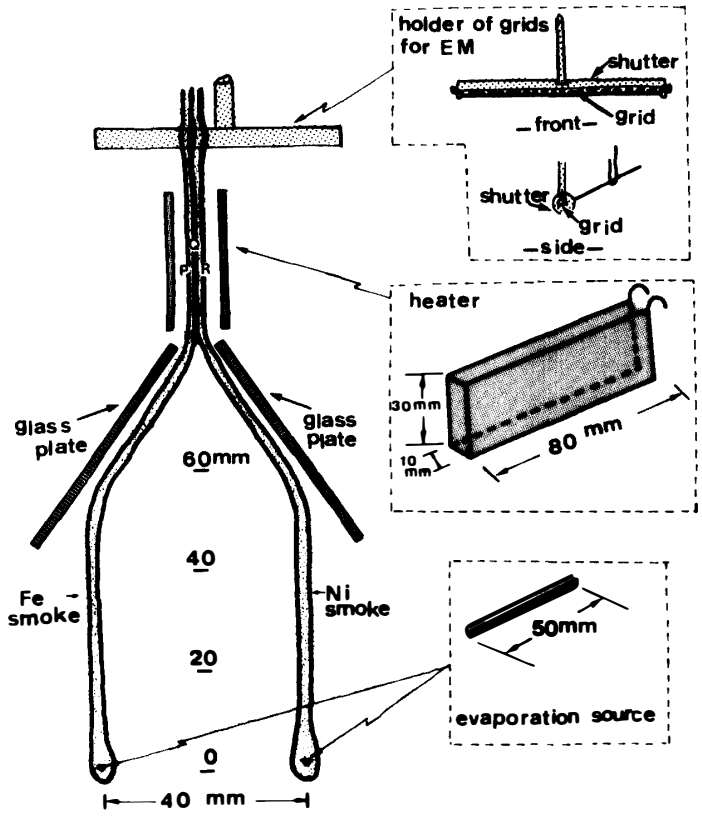

Fig. 2. Schematic illustration of coalescence growth instrumentation system. Fe and Ni ultrafine smoke grains are mixed and are passed through a heater, being finally collected on electron microscope grids located at Q.

with a stainless-steel plate on its top and a connector of a high-vacuum exhaust with a valve at its bottom. The two evaporation sources heated at 1700°C for Fe and Ni smokes are separated from each other by 40 mm in parallel in Ar gas of 13 kPa in pressure. Two glass plates ($80\times50\times1.5$ mm) are placed about 60 mm above the evaporation sources, with angle 60° to the vertical. The smoke streams rising straight up from the sources flow along the glass plates, and the joined smoke stream at the ends of glass plates flows straight upward again. A heater (80 mm long) made with a folded stainless steel net is placed for the joint smoke to pass through its gap (30 mm in height and 10 mm in width). Grain specimens are collected on an electron microscope grid placed 10 mm above the upper end of the heater, indicated by Q in Fig. 2.

Temperature of the joined smoke before heating by the heater is lower than 70°C. When the joined smoke is not heated up, no alloy grains are formed, Fe and Ni grains only being detected.

In the present study, the formation temperature of ordered alloy grains due to the coalescence process between Fe and Ni smoke grains is determined by examining the collected final grain specimens by an electron microscope HITACHI H-800, and X-ray microanalysis operated with an electron microscope, HITACHI H-9000, interfaced to KEVEX, an energy-dispersive X-ray analysis system.

Temperature within the gap of the heater is changed at intervals of every 50°C between 100°C and 450°C, and it is kept within $\pm$10°C in errors at every temperature step. In the grains which passed through the heater gap at temperatures higher than 200°C, presence of the ordered alloy grains is always definitely detected. It is also found that the coalescence production alloy grains formed on the Fe-smoke side (the

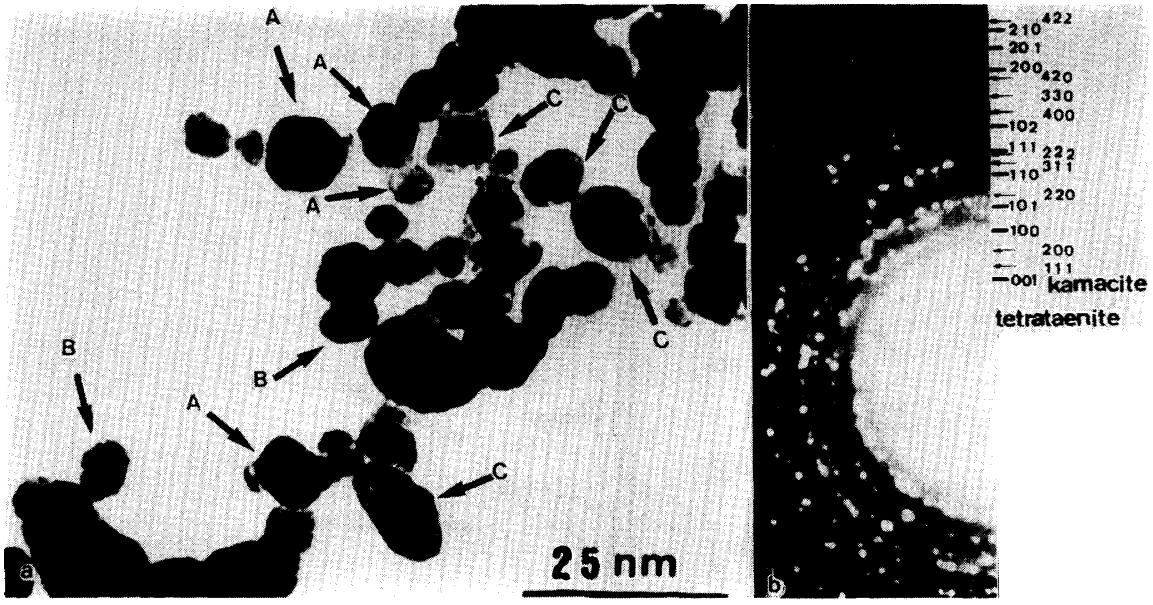

Fig. 3. EM images (left) and ED pattern (right) of the coalescence product grains collected on the grid collector at Q. Heater gap temperature=200°C. Arrows A, B, and C in EM pattern indicate respectively, square shape, polyhedral shape and double structure grains of Fe-Ni alloy. ED pattern is indexed as tetrataenite plus ordered kamacite.

left side in Fig. 2) and on the Ni-side are richer in Fe and Ni contents respectively. This result is in agreement with the result previously obtained for Bi_2O_3-MoO_3 system (KAITO, 1981).

Figure 3 shows an example of the electron microscope (EM) image and the corresponding electron diffraction (ED) pattern of the grains which passed through the heater gap of 200°C. Grains A, B and C in Fig. 3 (a) are of the shapes of square, polyhedral and a double structure having an enveloping layer, respectively. The ED patterns in Fig. 3(b) present both the ordered structure of tetrataenite which has a crystal structure shown by Fig. 4(b) and the ordered structure of Fe_3Al type having kamacite composition (Fe_3Ni) which is shown by Fig. 4(a). Fig. 4(c) is the crystal structure of awaruite ($FeNi_3$).

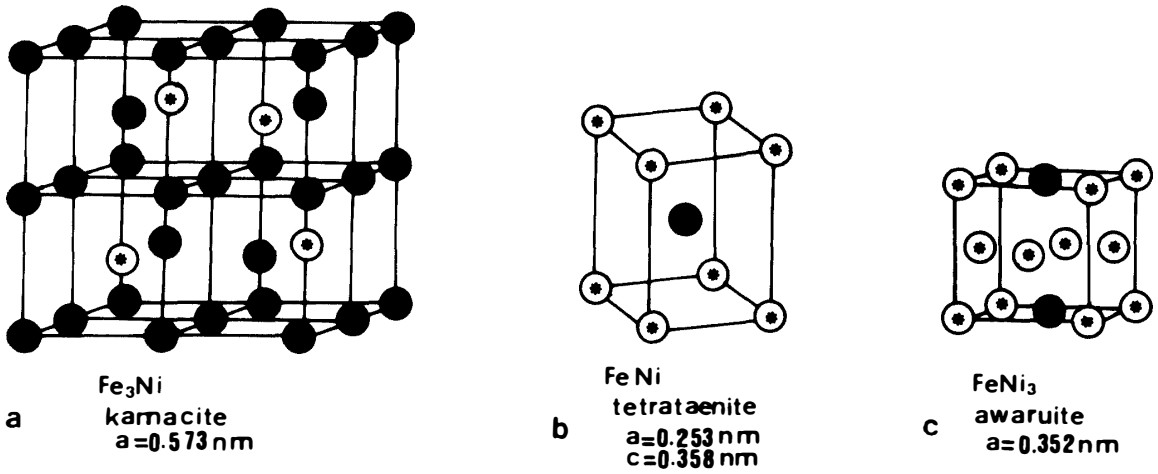

Fig. 4. Three ordered crystal structures of Fe-Ni system. (a) ordered kamacite. (b) tetrataenite. (c) awaruite.

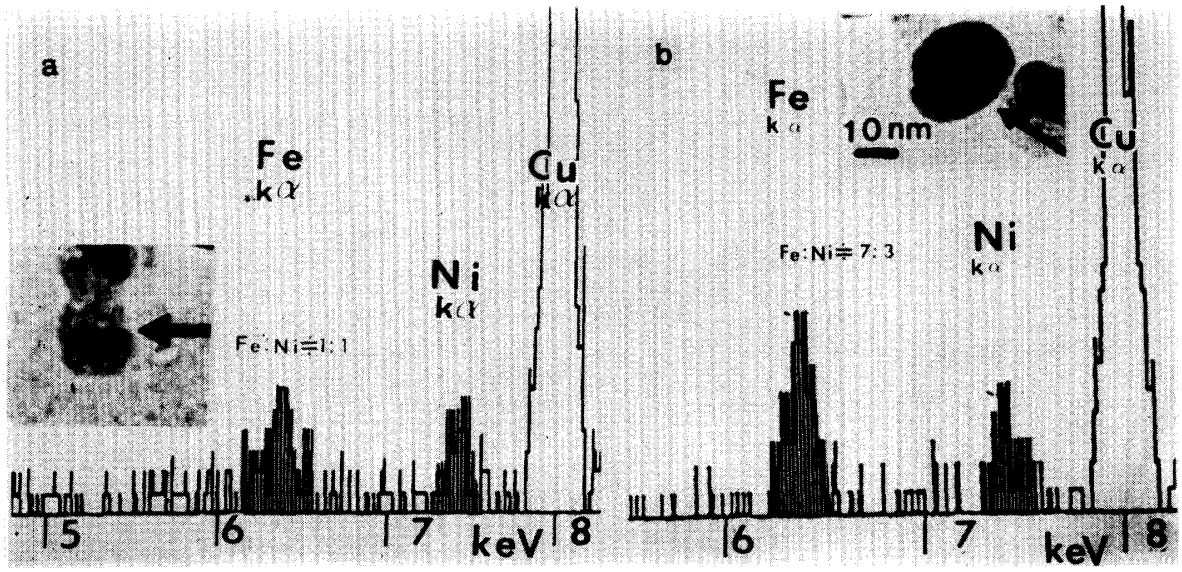

Fig. 5. X-ray spectra of coalescence growth product grains. Left (a): tetrataenite. Right (b): ordered kamacite.

The X-ray spectrum of the square shape grain (tetrataenite) is shown in Fig. 5a. Since a difference of the characteristic energy of KαX-ray between Fe and Ni is negligibly small in the first approximation, the observed Kα intensity ratio I(Fe): I(Ni)= 52: 48 may chemically well represent the tetrataenite phase. Figure 5b gives the X-ray spectrum of the grain of B-type shown in Fig. 3a. The X-ray spectrum indicates that the chemical composition of the grain can be approximately expressed by $Fe_{72}Ni_{28}$, which is roughly equal to the composition of Fe_3Ni kamacite. Since the multiple scatterings of electron and radiated X-ray hardly take place in ultrafine grains, the above-mentioned approximation on the X-ray intensity ratio may be considered reasonable. The Cu lines in Fig. 5 are caused by a standard supporting grid.

Figure 6 shows the X-ray spectrum of a grain of C-type classified in Fig. 3. The composition of a square-shape central region is approximated to be given by $Fe_{51}Ni_{49}$, while the outer layer by $Fe_{69}Ni_{31}$. Since the superlattice part is observed, it could be concluded that the central part is identified to tetrataenite and the outer layer to ordered kamacite. Other type grains composed of the central part of ordered kamacite and the outer layer of tetrataenite also have been observed. With an increase in the heater temperature, larger ordered alloy grains are produced. Typical examples of ordered kamacite, tetrataenite and awaruite grains produced at 400°C in the heater temperature are shown in Fig. 7. It will be observed that ordered kamacite, tetrataenite and awaruite grains are of a complicated polyhedral shape, cubic one and rod-type one, respectively.

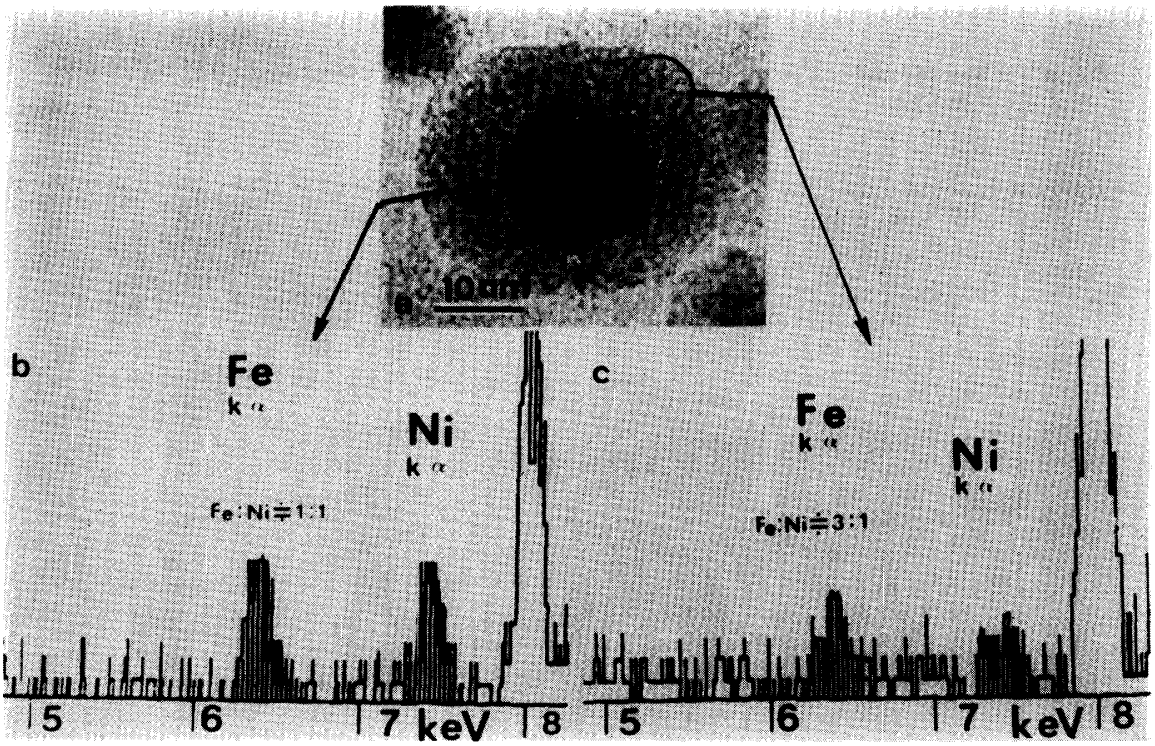

Fig. 6. X-ray spectrum of a double structure grain of Fe-Ni alloy. The central part is tetrataenite phase, while the outer layer is ordered kamacite.

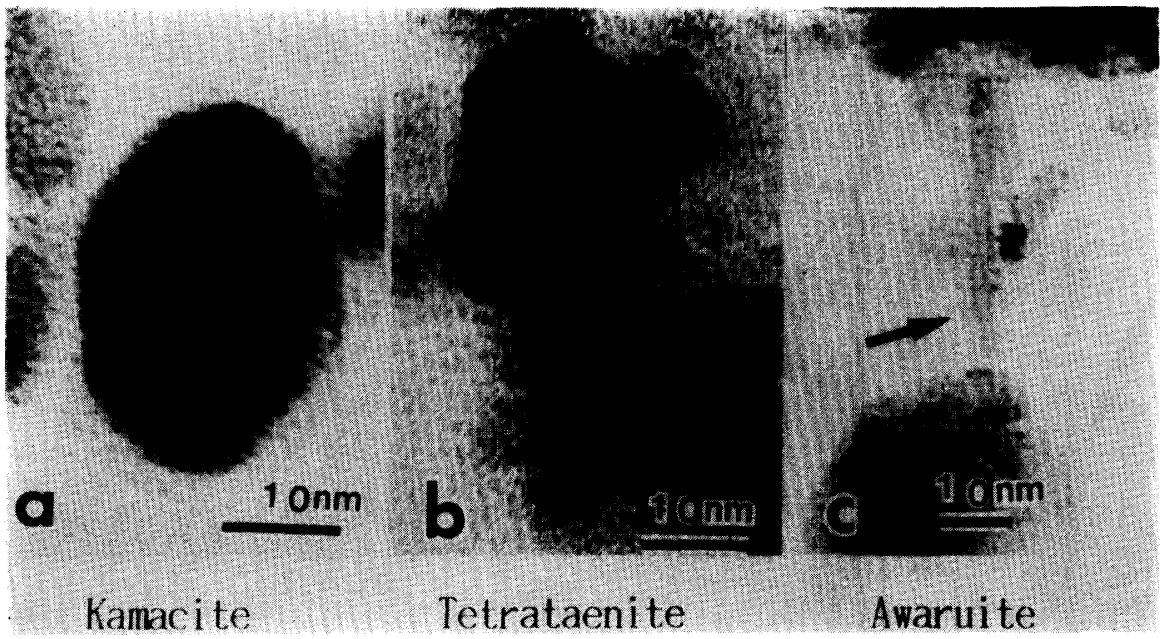

Fig. 7. Typical ordered structure grains produced in the present experimental system. (a) ordered kamacite. (b) tetrataenite. (c) awaruite.

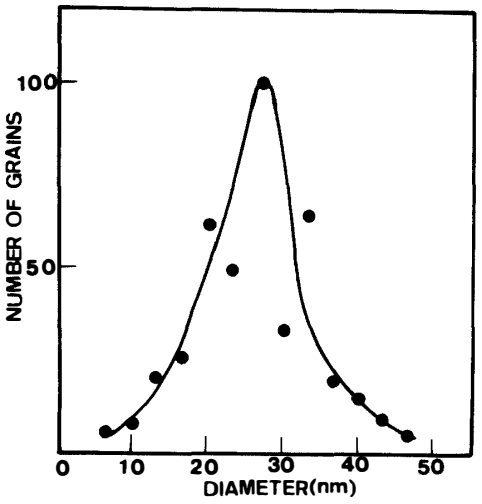

Fig. 8. Grain size distribution of ordered Fe-Ni alloy grains produced by the coalescence growth between Fe and Ni smoke flows at 250°C. (Total number of measured grains = 380. The peak value of the distribution is normalized to be 100.)

Figure 8 shows a typical example of the size distribution spectrum of ordered Fe-Ni alloy grains produced by the coalescence process of Fe and Ni smoke grains at 250°C. The grain size is determined on EM images of grains, where the grain size is defined as the mean outermost diameter of individual grains. The median value of grain size is 26 nm in diameter in this example.

As shown in Figs. 3, 5, 6, 7 and 8, it is experimentally demonstrated that fine tetrataenite grains of 10 nm or smaller in mean diameter can be produced by the coalescence process of Fe and Ni smoke grains at appropriate temperatures. This result may suggest that fine grains in chondritic meteorites might possibly be formed by a similar coalescence process of Fe gas and Ni gas in the early solar nebula. This

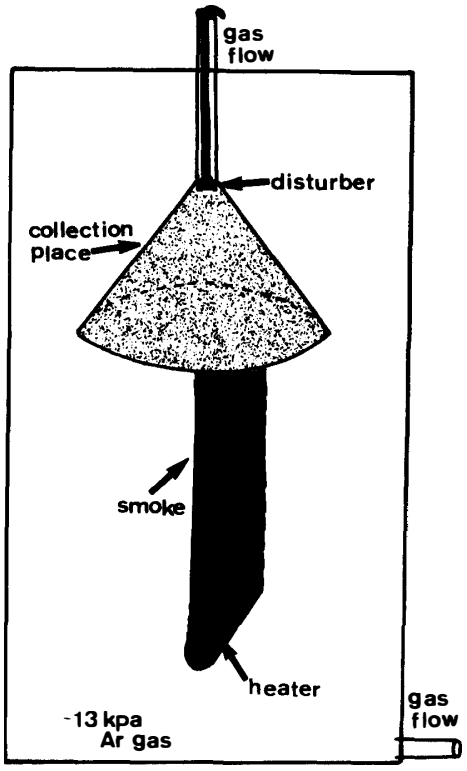

Fig. 9. Schematic illustration of coalescence product sample collector parts for the purpose of collecting a larger amount of coalescence growth product grains (see text).

process could be considered as the primary formation hypothesis of fine tetrataenite grains in chondrites.

On the other hand, it has been demonstrated that fine tetrataenite grains are produced by evaporating a taenite mass of $Fe_{50}Ni_{50}$ composition in Ar gas atmosphere of 13 kPa pressure (KAITO *et al.*, 1989). There may be present a possibility, therefore, that fine tetrataenite grains in chondrites were formed by an appropriate evaporation process of the ordinary disordered taenite having approximate composition of $Fe_{50}Ni_{50}$. This secondary formation hypothesis also cannot be rejected. In the present study, the sample collection system for the grains of coalescence production is modified for the purpose of getting a larger amount of the ordered Fe-Ni alloy grains to be examined in more detail with various experimental techniques. Figure 9 illustrates a schematic view of the modified sample collection system. After evacuating the inside of the chamber, Ar gas of about 13 kPa pressure continuously flows from the bottom to the top in the chamber associated with convective and turbulent motions, too. The evaporation heater of Fe-Ni grains is a tungsten V-boat of 50 mm in length, 2 mm in width and 1 mm in depth, heated at $1600 \sim 1900$°C. When a larger size of the evaporating sample boat is adopted, the collected coalescence product scarcely contains the ordered Fe-Ni grains, as described later. Evaporated smoke grains rising upward with the convecting flow of Ar gas tend to converge within a glass funnel attached by a small disturber to produce turbulent motions of the smoke within the funnel. Thus, a considerably large amount of the coalescence production grains is accumulated on the inner surface of the funnel.

Figure 10a shows an example of grain shape and X-ray diffraction pattern of

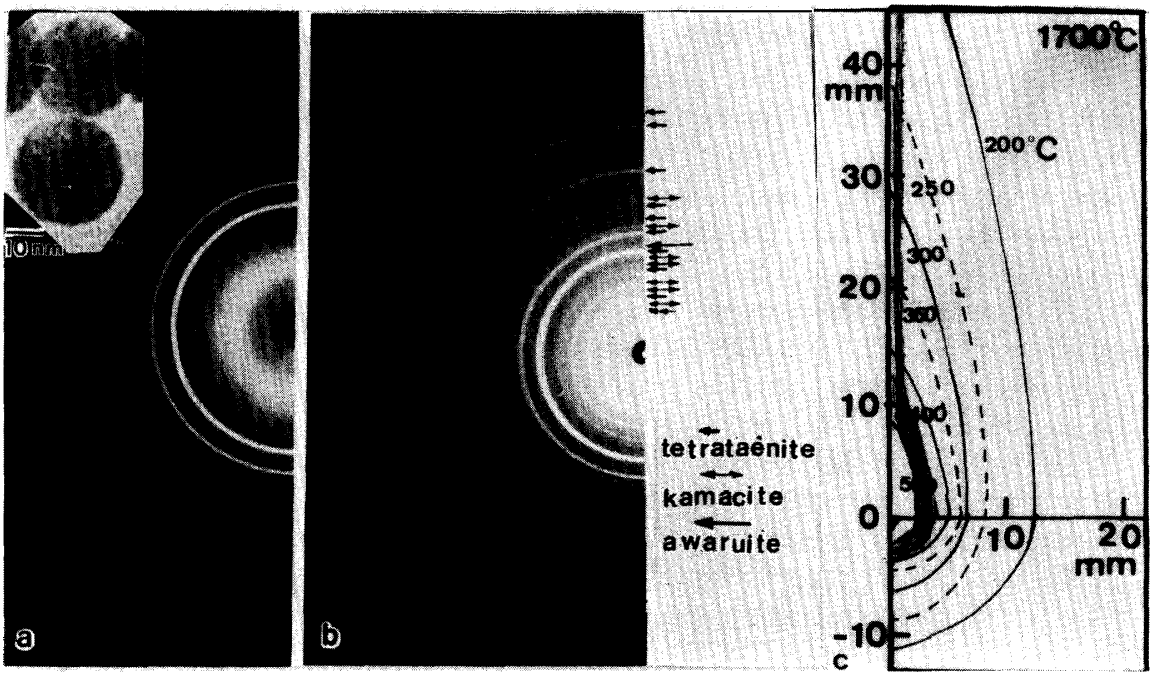

Fig. 10. (*a*) *X-ray diffraction patterns of disordered phase of Fe-Ni alloy grains, which have a spherical shape.*
(*b*) *X-ray diffraction patterns of ordered phases of Fe-Ni alloy grains.*
(*c*) *Temperature distribution in smoke flow evaporated from Fe-Ni alloy to produce coalescence growth products of ordered Fe-Ni grains* (*see text*).

disordered taenite, which occupies almost all of the coalescence product grains in the case that $Fe_{50}Ni_{50}$ metal is evaporated in a large source boat at 1700°C. Figure 10b shows X-ray diffraction pattern of the collected sample produced by evaporating $Fe_{50}Ni_{50}$ disordered grain source in the standard source boat at 1700°C. The coalescence product contains tetrataenite, awaruite and ordered kamacite.

Figure 10c illustrates the temperature distribution in the upward flowing evaporation smoke on the best condition to produce the ordered Fe-Ni grains in the collected coalescence product specimens. It may be empirically concluded that about 500°C of the smoke temperature near the evaporation source gives rise to the largest efficiency in producing the ordered Fe-Ni grains by the coalescence process. The temperature distribution can be surveyed only with a special alumel-chromel thermojunction of 20 μm in diameter (KAITO, 1978).

Another empirical finding is that the synthesized evaporation source alloy grains of $Fe_{45}Ni_{55}$ composition can produce considerably more tetrataenite by the coalescence process than any other evaporation source compositions such as $Fe_{50}Ni_{50}$ and Fe_{55}-Ni_{45}.

It seems likely that there still remain a number of problems in coalescence phenomena between Fe and Ni. More quantitative studies on this phenomenon, such as coalescence interaction between a thin film of Fe and a small spherical particle of Ni, or a thin film of Ni and a small spherical particle of Fe, are under way at present.

4. Magneitc Properties of Tetrataenite Grains Produced by Coalescence Process

Magnetic properties of the coalescence product grains obtained from evaporating synthesized $Fe_{50}Ni_{50}$ grains are examined. It was confirmed by X-ray analyses before the magnetic measurements that the test samples contain tetrataenite of more than a half of the total metal volume together with other Fe-Ni alloy phases. The magnetic test samples are of a form of a uniform mixture of the coalescence product grains with SiO_2 powders, sealed into a thin silica tube.

An example of the first run thermomagnetic cycle curves of the test sample in a magnetic field of $H_{ex}=10$ kOe is shown in Fig. 11. The second run thermomagnetic cycle curves are almost thermally reversible and practically identical to the first run cooling curve.

As shown in the figure, the first run cooling thermomagenetic curve well represents the reversible thermomagnetic curve of disordered taenite of about $Fe_{50}Ni_{50}$ composition, no trace of presence of the ordinary disordered kamacite being detectable. The first run heating thermomagnetic curve reasonably well represents a destruction of the tetrataenite phase and its transformation to disordered taenite at temperature

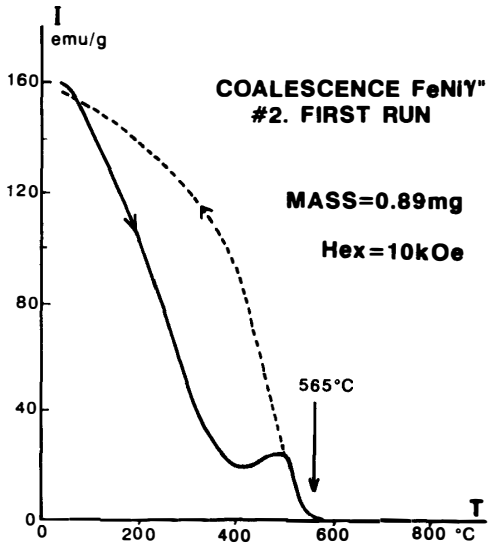

Fig. 11. First run thermomagnetic cycle curves of coalescence growth product Fe-Ni grains.

Table 3. Magnetic hysteresis parameters of coalescence product Fe-Ni grains.

	Sample #2 (0.01 mg)				Sample #3 (0.32 mg)			
	Original		After heating		Original		After heating	
I_S (emu/g)	161		153		178		124	
I_R (emu/g)	48.2		0.7		58.0		0.6	
H_C (Oe)	305		6		460		5	
H_{RC} (Oe)	516		47		787		70	
Composition	γ	γ'	γ	γ'	γ	γ'	γ	γ'
(wt%)	35	65	100	~0	40	60	100	~0

below about 400°C. (For reference, the thermomagnetic curves of ultrafine tetrataenite grains contained in the silicate grains of the matrix of St. Séverin chondrite also have nearly the same characteristics (NAGATA and FUNAKI, 1989)).

Table 3 summarizes the measured values of magnetic hysteresis parameters at 28~30°C of two test samples before and after twice heatings up to 800°C in vacuum (5×10^{-5} Torr). As shown in the table, I_R and H_C values are drastically reduced after the heat treatment, indicating that the high coercivity component, tetrataenite, is almost completely destructed. Although a numerically reliable determination of the coercive force ($H_C^{(h)}$) of the high coercivity component is difficult, because the observed H_{RC}/H_C value is as small as close to that of an anisotropic single domain ferromagnetic particle (*e. g.*, NAGATA and CARLETON, 1987) in the present case, it is certain that $H_C^{(h)}$ is only a little larger than the measured value of H_C for the present test samples. In other words, it seems that $H_C^{(h)}=300\sim500$ Oe for the test samples is too small in comparison with the standard value $H_C=2000\sim2500$ Oe for a random oriented ensemble of tetrataenite particles. This result may be interpreted as due to a dominant presence of tetrataenite nucleus grain enveloped by a low coercivity layer, such as the double structure grains shown in Fig. 3, because the enveloping low coercivity layer results in a decrease of the total average coercivity. In tetrataenite-rich chondrites also, an apparent low coercivity force of tetrataenite phase has been found, such as Y-74160 LL7 chondrite for example (NAGATA and FUNAKI, 1982). Such a possible interpretation as described above should be examined more definitely in the future studies.

Figure 12 shows a dependence of the weight content of ferromagnetic tetrataenite phase in #3 test sample (mass of Fe-Ni metal=0.89 mg) of the same coalescence product on temperature below 25°C, for the purpose of granulometry of tetrataenite phase grain. As shown in the figure, tetrataenite grains larger than 7 nm in mean diameter are about 40 wt% and those smaller than 7 nm are also about 40 wt%, the remaining magnetic grains of about 20 wt% could be identified to disordered

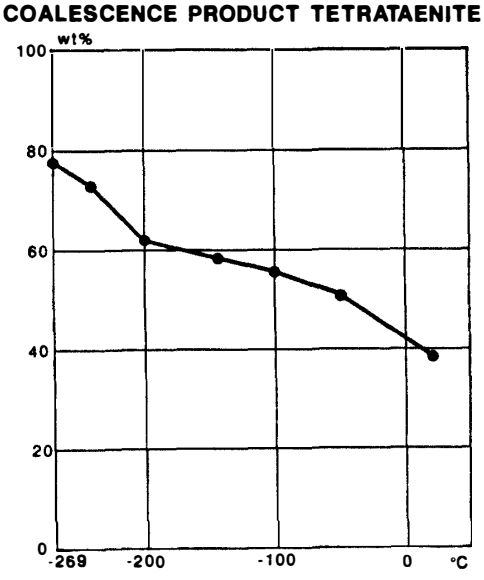

Fig. 12. Bulk content of ferromagnetic tetrataenite at low temperatures in coalescence growth product ordered Fe-Ni grains produced from evaporated disordered $Fe_{50}Ni_{50}$ sample.

taenite in the original condition.

5. Concluding Remarks

In the present experimental works, two main points regarding tetrataenite are specifically examined. They are; (1) magnetic analyses, in association with EMPA chemical ones and Mössbauer spectral ones, of Fe-Ni grains in chondritic meteorites, have revealed that chondrites often contain fine tetrataenite grains of 10 nm or smaller in mean diameter, and (2) laboratory experiments can demonstrate the formation of tetrataenite fine grains by the coalescence growth at 200～500°C temperature, from either (a) a joint cloud of evaporated smoke flows of Fe and Ni or (b) a Fe-Ni smoke cloud evaporated from relatively large disordered taenite grains of $Fe_{50}Ni_{50}$ composition. These two results may lead to a possibility that tetrataenite grains in unequilibrated chondrites might be formed with the process of coalescence growth of Fe and Ni ultrafine particles in the early solar nebula at appropriate temperatures. There might also be another possibility that tetrataenite fine grains in some chondrites were formed with the process of coalescence growth of particle smokes of Fe+Ni which were evaporated caused by some explosive event from disordered taenite metals of $Fe_{50}Ni_{50}$ in roughly approximate composition in existing planetesimals.

So far as tetrataenite fine grains produced by the present coalescence growth experiments are concerned, however, it seems very likely that the majority of individual tetrataenite grains have a double phase structure consisting of a magnetically much less coercive Fe-Ni alloy, such as kamacite and/or disordered taenite in addition to pure tetrataenite, thus resulting in a considerable reduction of magnetic coercivity as a whole. Since fine grains of almost pure tetrataenite are commonly present in chondrites, a problem whether fine grains of such pure tetrataenite can be produced by the coalescence growth process on appropriate conditions will have to be studied in future.

This research work is supported, in part, by a special research grant from the Ministry of Education, Science and Culture of Japan, No. 132410011389, and in part by a research fund from the Japan Academy.

References

CHAMBEROD, A., LAUGIER, J. and PENISSON, J. M. (1979): Electron irradiation effects on iron-nickel invar alloys. J. Magn. Magn. Mineral., **10**, 139–144.

DANON, J., SCORZALLI, R. B., SOUZA AZEVEDO, J. and CRISTOPHE MICHEL-LEVY, M. (1979): Iron nickel superstructure metal particles. Nature, **281**, 469–471.

KAITO, C. (1978): Coalescence growth of smoke particles prepared by a gas-evaporation technique. Jpn. J. Appl. Phys., **17**, 601–609.

KAITO, C. (1981): Formation of double oxides by coalescence of smoke particles of different oxides. J. Cryst. Growth, **55**, 273–280.

KAITO, C. (1984): Electron microscopic study of the alloy particles produced by coalescence of Au and Cu smokes. Jpn. J. Appl. Phys., **23**, 525–528.

KAITO, C. (1985): Coalescence growth mechanism of smoke particles. Jpn. J. Appl. Phys., **24**, 261–264.

KAITO, C. and SAITO, Y. (1989): Ordered grains produced by coalescence of Fe and Ni smoke grains.

Proc. Jpn. Acad., **65**, Ser. B, 125–128.

KAITO, C., SAITO, Y. and FUJITA, K. (1989): Ordered structure in alloy grains of iron-nickel produced by the gas evaporation technique. Jpn. J. Appl. Phys., **28**, L694–L696.

KIMOTO, K., KAMIYA, Y., NONOYAMA, M. and UYEDA, R. (1963): An electron microscope study of fine metal particles prepared by evaporation in argon gas at low pressure. Jpn. J. Appl. Phys., **2**, 702–713.

NAGATA, T. (1961): Rock Magnetism (Rev. ed). Tokyo, Maruzen, 350 p.

NAGATA, T. (1988): Magnetic analysis of Antarctic chondrites on the basis of a magnetic binary system model. Proc. NIPR Symp. Antarct. Meteorites, **1**, 247–262.

NAGATA, T. and CARLETON, B. J. (1987): Magnetic remanence coercivity of rocks. J. Geomagn. Geoelectr., **39**, 447–461.

NAGATA, T. and CARLETON, B. J. (1989): Tetrataenite in chondritic meteorites. Proc. Jpn. Acad., **65**, Ser. B, 121–124.

NAGATA, T. and FUNAKI, M. (1982): Magnetic properties of tetrataenite-rich stony meteorites. Mem. Natl Inst. Polar Res., Spec. Issue, **25**, 222–250.

NAGATA, T. and FUNAKI, M. (1987): Tetrataenite phase in Antarctic meteorites. Mem. Natl Inst. Polar Res., Spec. Issue, **46**, 245–262.

NAGATA, T. and FUNAKI, M. (1989): Magnetic analysis of Antarctic ordinary chondrites and achondrites on the basis of a magnetic binary system model. Proc. NIPR Symp. Antarct. Meteorites, **2**, 310–325.

NAGATA, T., FUNAKI, M. and DANON, J. A. (1986): Magnetic properties of tetrataenite-rich meteorites, II. Mem. Natl Inst. Polar Res., Spec. Issue, **41**, 364–386.

NAGATA, T., DANON, J. A. and FUNAKI, M. (1987): Magnetic properties of Ni-rich iron meteorites. Mem. Natl Inst. Polar Res., Spec. Issue, **46**, 263–282.

NÉEL, L. (1949): Théorie du trainage magnétique de ferromagnétique aux grains fins avec applications aux terres cuites. Ann. Geophys., **5**, 99–136.

NÉEL, L. (1955): Some theoretical aspects of rock magnetism. Philos. Mag. Suppl. Adv. Phys., **4**, 191–243.

NÉEL, L., PAULEVE, J., PAUTHENET, R., LUGIER, J. and DAUTREPPE, D. (1964): Magnetic properties of an iron-nickel single crystal ordered by neutron bombardment. J. Appl. Phys., **35**, 873–877.

SCHWERE, F. C. and NAGATA, T. (1976): Ferromagnetic-superparamagnetic granulometry of lunar surface materials. Proc. Lunar Sci. Conf., 7th, 759–778.

SCOTT, V. D. and LOVE, G. (1983): Quantitative Electron Probe Microanalysis. Chichester, Ellis Harwood, 345 p.

(*Received August 16, 1990; Revised manuscript received January 10, 1991*)